Electronic Supplementary Information

The Near-UV Absorber OSSO and Its Isomers

Zhuang Wu,[a] Huabin Wan,[a] Jian Xu,[a] Bo Lu,[a] Yan Lu,[a] André K. Eckhardt,[b] Peter R. Schreiner,*[b]

Changjian Xie,[c] Hua Guo,[c] and Xiaoqing Zeng*[a]

[a]College of Chemistry, Chemical Engineering and Materials Science, Soochow University, Suzhou

215123 China; E-mail: xqzeng@suda.edu.cn

[b]Institute of Organic Chemistry, Justus-Liebig University, Heinrich-Buff-Ring 17, 35392 Giessen,

Germany; E-mail: prs@uni-giessen.de

[c]Department of Chemistry and Chemical Biology, University of New Mexico, Albuquerque, NM

87131, USA

Table of Contents:

Experimental details

Sample preparation. Ethylene episulfoxide were prepared according to the published protocols[1]. The purity was checked by using ^1H and ^{13}C NMR spectroscopy (Bruker Avance III HD 400 spectrometer). Ar ($\geq$ 99.999%, Messer) and N_2 ($\geq$ 99.999%, Messer) gases were used without further purification. 5-Methyl-1,3,4-oxthiazol-2-one was prepared according to literature.[2]

Matrix-isolation IR spectroscopy. Matrix IR spectra were recorded on a FT-IR spectrometer (Bruker 70V) in a reflectance mode by using a transfer optic. A KBr beam splitter and liquid-nitrogen cooled broadband MCT detector were used in the mid-IR region (4000–400 cm^{-1}). Typically, 200 scans at a resolution of 0.5 cm^{-1} were co-added for each spectrum. Gaseous ethylene episulfoxide was mixed by passing a flow of Ar or N_2 gas through a U-trap containing ca. 20 mg of ethylene episulfoxide at –27 °C or 5-methyl-1,3,4-oxthiazol-2-one at –28 °C. Then the mixture (estimated ratio of 1:1000) was passed through an aluminum oxide furnace (o.d. 2.0 mm, i.d. 1.0 mm), which can be heated over a length of ca. 25 mm by a tantalum wire (o.d. 0.4 mm, resistance 0.4 Ω), deposited (2 mmol h^{-1}) in a high vacuum (~10^{-6} pa) onto the Rh-plated Cu block matrix support (15.0 K for Ar and N_2) using a closed-cycle helium cryostat (Sumitomo Heavy Industries, SRDK-408D2-F50H) inside the vacuum chamber. Temperatures at the second stage of the cold head were controlled and monitored using a LakeShore 335 digital cryogenic temperature controller a Silicon Diode (DT-670). The voltage and current used in the pyrolysis experiments are 5.0 V and 3.45 A, respectively. Photolysis experiments were performed using an Nd^{3+}: YAG laser (266 and 532 nm, MPL-F-266, 10 mW), and UV flashlight (365 nm, Boyu T648, 20 W).

Matrix-isolation UV/Vis spectroscopy.

The cryostat used was an APD Cryogenics HC-2 closed-cycle refrigerator system with BaF_2 window for UV/Vis measurements. UV/Vis spectra with a Jasco V670 spectrometer (spectral range of 190–850 nm with a scanning speed of 1 nm s^{-1}). For the combination of high-vacuum flash pyrolysis with matrix isolation, a small, home-built, water-cooled oven directly connected to the vacuum shroud of the cryostat was used. The pyrolysis zone consisted of a completely empty quartz tube (inner diameter 8 mm, length of heating zone 50 mm) resistively heated by a coax heating wire. The temperature was controlled through a Ni/CrNi thermocouple. A gas mixture of ethylene episulfoxide and Ar (1:1000) was prepared in a 2 L storage bulb and evaporated at room temperature into the quartz pyrolysis tube. Immediately after leaving the tube, at a distance of ca. 50 mm, all pyrolysis products were condensed (typically 30 to 60 mbar in one hour) on the surface of the 12.0 K matrix window. For irradiation UV light (365 nm), and low-pressure mercury lamp (254 nm) were used.

Computational details

Molecular structures and IR frequencies of stationary points were computed using UB3LYP/6-311+G(3df)[3] and UCCSD(T)-F12b/VTZ-F12.[4] Local minima were confirmed by vibrational frequency analysis. The time-dependent TD-B3LYP method was performed for the prediction of vertical excitations.[5] These computations were performed using the Gaussian 09 software package.[6] The CCSD(T)-F12 computations were performed using the MOLPRO[7] packages.
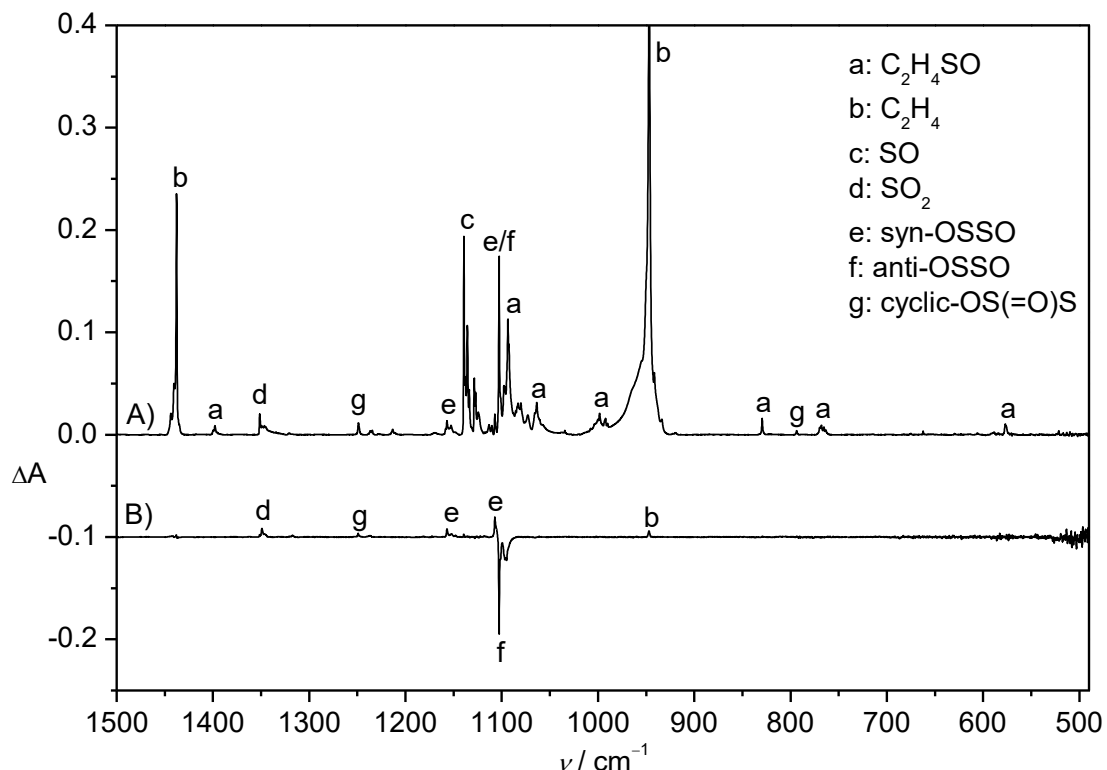
**Figure S1.** A) IR spectrum of matrix isolated HVFP (1000 K) products of ethylene episulfoxide (**a**) in N_2 (1:1000) at 15 K. B) IR difference spectrum reflecting the change of the same matrix upon green light irradiation (532 nm, 25 min).
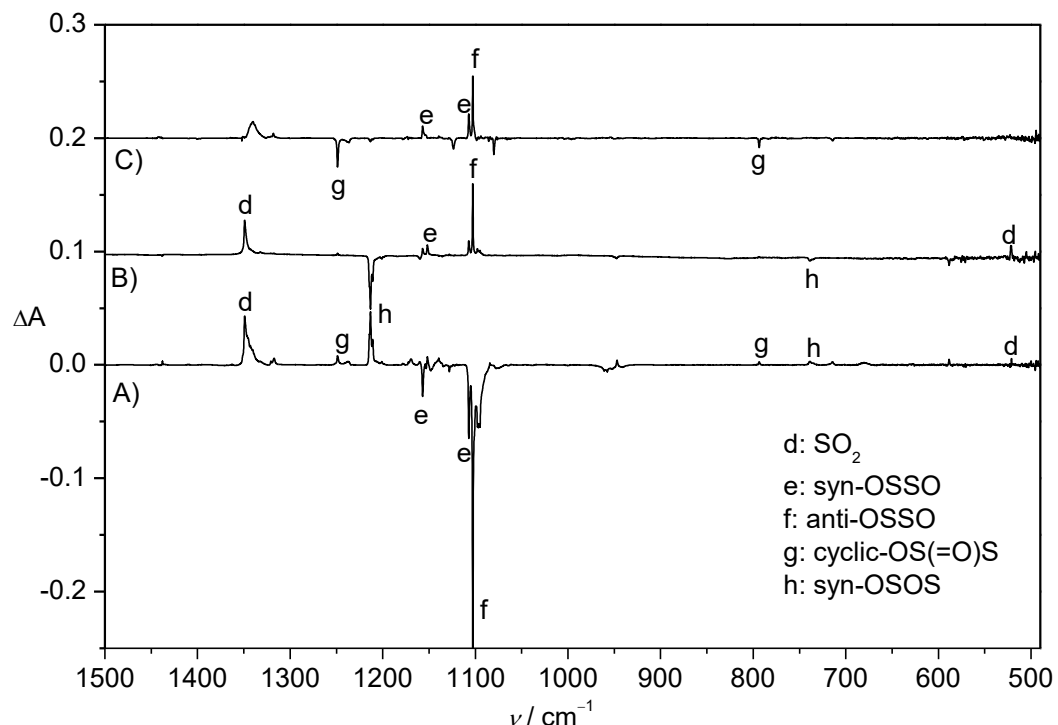
Figure S2. A) IR difference spectrum reflecting the depletion of **e** and **f** and the formation of **d, g,** and **h** upon UV light irradiation (365 nm, 5 min) in solid N_2 matrix. B) IR difference spectrum reflecting the depletion of **h** and the formation of **d, e**, and **f** upon green light irradiation (532 nm, 5 min). C) IR difference spectrum reflecting the depletion of **g** and the formation of **e** and **f** upon UV light irradiation (266 nm, 8 min).
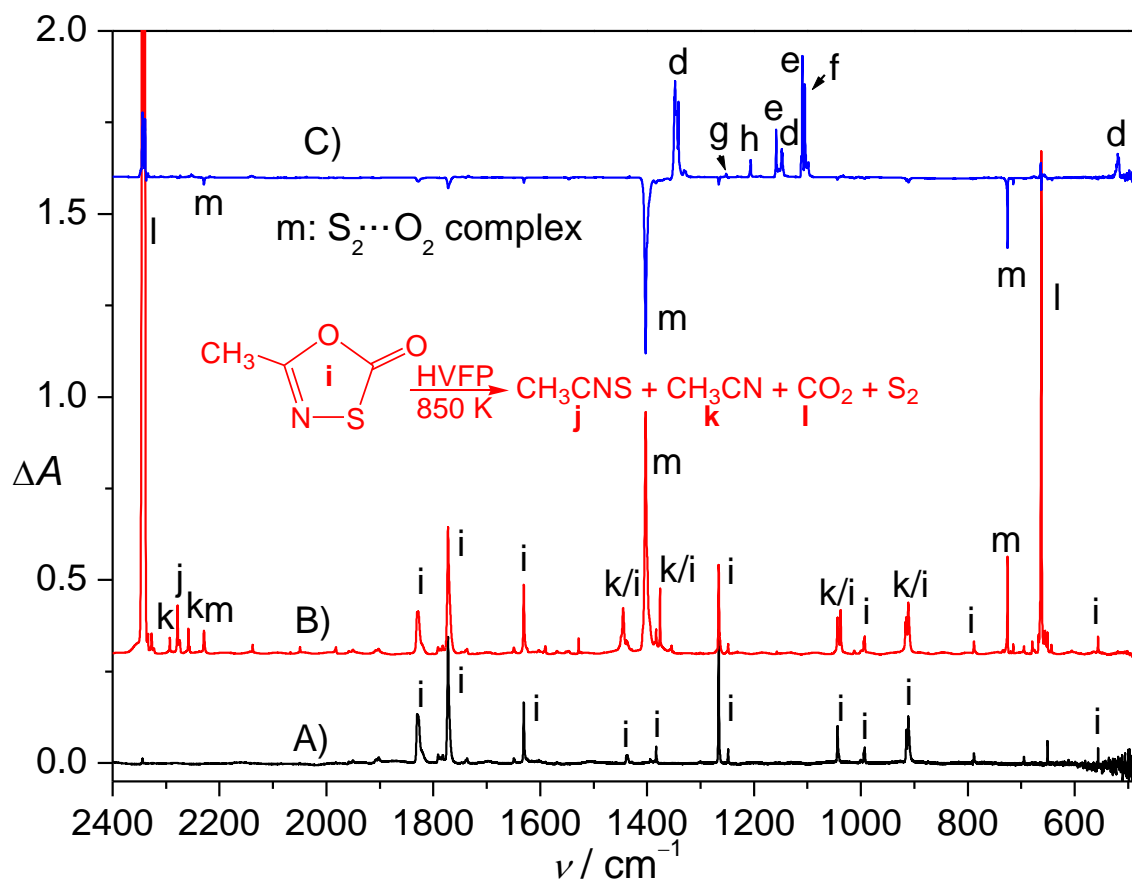
Figure S3. A) IR spectrum of matrix isolated 5-methyl-1,3,4-oxthiazol-2-one (i) in solid Ar matrix (1:1000) at 15 K. B) HVFP (850 K) products of 5-methyl-1,3,4-oxthiazol-2-one (i) in Ar (1:1000) at 15 K. C) IR difference spectrum reflecting the depletion of **m** and the formation of SO_2 (d) and S_2O_2 isomers (**e**, **f**, **g**, and **h**) upon UV light irradiation (266 nm, 22 min). The pyrolysis of 5-methyl-1,3,4-oxthiazol-2-one (i) has been studied in literatures.[8]
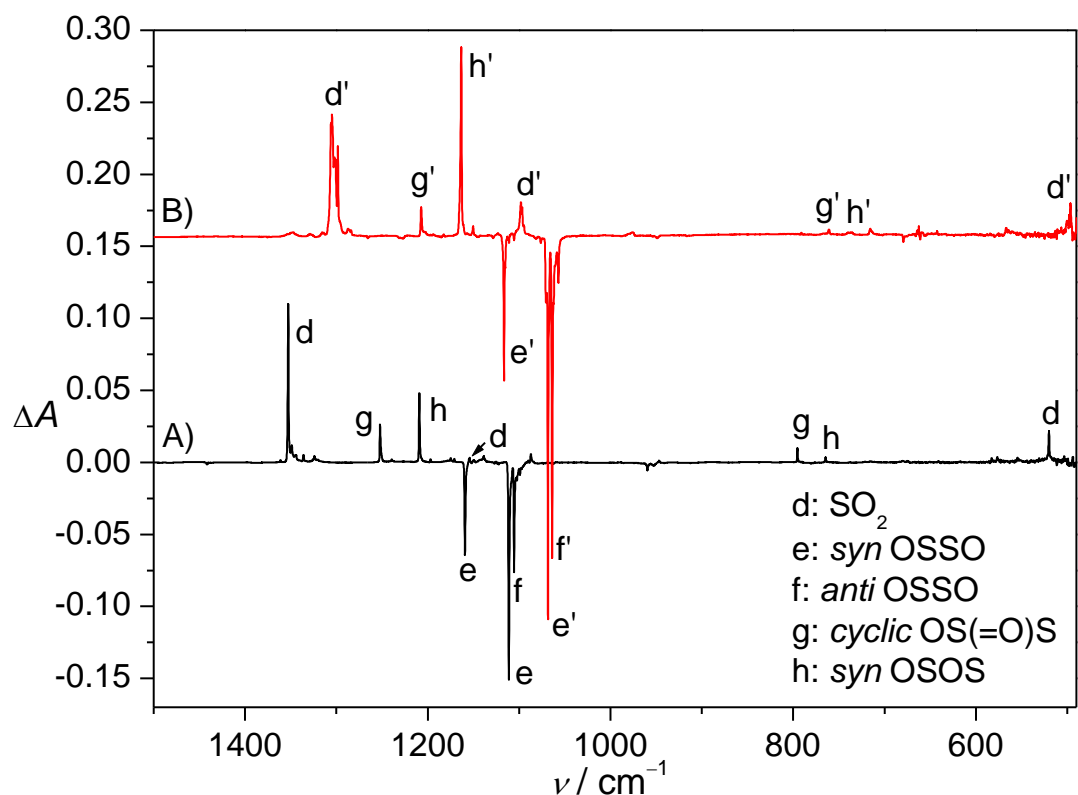
Figure S4. A) IR difference spectrum reflecting the depletion of **e** and **f** and the formation of **d**, **g**, and **h** upon UV light irradiation (365 nm, 5 min); B) IR difference spectrum reflecting the depletion of doubly-^{18}O labeled **e** and **f** and the formation of **d**, **g**, and **h** upon UV light irradiation (365 nm, 5 min).
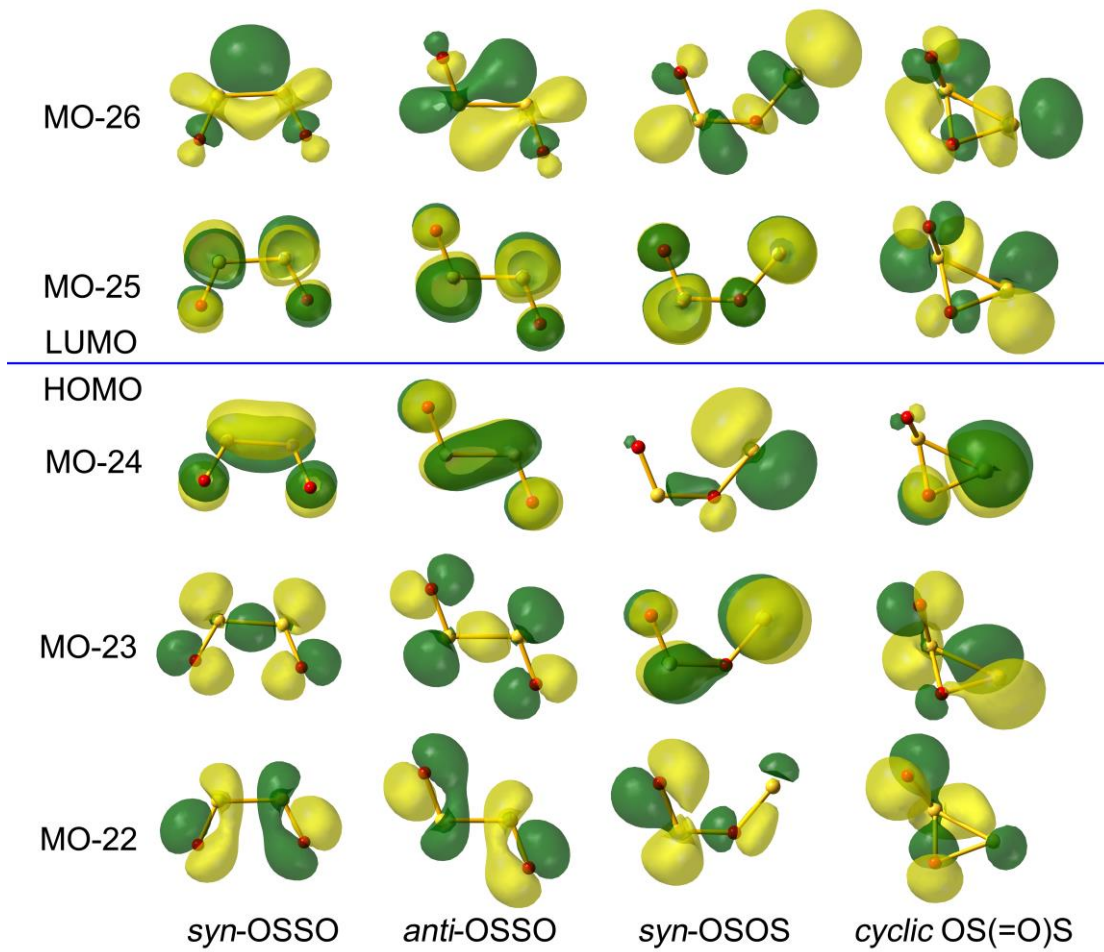
Figure S5. Frontier molecular orbitals of S_2O_2 isomers computed at the B3LYP/6-311+G(3df) level.

Table S1. TD-DFT B3LYP/6-311+G(3df) calculated spin-allowed vertical excitation energy (> 230 nm) of S_2O_2 isomers.

species	energy (nm)	oscillator strength (*f*)	main contribution
syn-OSSO	495	0.0000	MO-23 → MO-25
	350	0.0706	MO-24 → MO-25
	306	0.0000	MO-24 → MO-26
	281	0.0034	MO-23 → MO-26
	256	0.0005	MO-22 → MO-25
anti-OSSO	542	0.0000	MO-23 → MO-25
	400	0.0698	MO-24 → MO-25
	295	0.0000	MO-24 → MO-26
	264	0.0005	MO-22 → MO-25
	261	0.0060	MO-23 → MO-26
syn-OSOS	1190	0.0000	MO-24 → MO-25
	436	0.1453	MO-23 → MO-25
	334	0.0120	MO-24 → MO-26
	314	0.0000	MO-23 → MO-26
	286	0.0016	MO-22 → MO-25
	232	0.0153	MO-24 → MO-27
cyclic OS(=O)S	451	0.0001	MO-24 → MO-25
	339	0.0012	MO-24 → MO-26
	257	0.0265	MO-23→ MO-25
	244	0.0381	MO-23→ MO-26
	233	0.0300	MO-22→ MO-25

Table S2. Computed and observed IR frequencies (cm^{-1}) of *syn*-OSSO.

computed[a]							observed[d]			mode
B3LYP/6-311+G(3df)		CCSD(T)-F12b/ VTZ-F12		MRCI/ cc-pV(T+d)Z[b]	fc-CCSD(T)/ cc-pV(Q+d)Z[c]					
normal	guess=mix	harmonic	anharmonic	harmonic	harmonic	anharrmonic	Ar-matrix	N$_2$-matrix	Ne-matrix	
1192 (71)	1192 (71)	1191	1173 (125)	1288 (110)	1187	1171 (47)	1159.3 (100)	1157.1 (100)	1162.8 (100)	ν_1
1139 (228)	1139 (228)	1139	1122 (738)	1234 (300)	1137	1120 (165)	1112.5 (38)	1107.2 (46)	1115.4 (31)	ν_2
490 (1)	490 (1)	492	482 (1)	526 (<1)	487	478 (0.3)				ν_3
475 (18)	475 (18)	476	471 (40)	505 (49)	475	470 (17)				ν_4
286 (0)	286 (0)	279	275 (0)	275 (0)	277	274 (0)				ν_5
138 (5)	138 (5)	134	136 (8)	162 (9)	130	131 (5)				ν_6

[a] Computed IR intensities (km mol^{-1}) in parentheses. [b] B. N. Frandsen, P. O. Wennberg, H. G. Kjaergaard, *Geophys. Res. Lett.* **2016**, *43*, 11146–11155. [c] M. A. Martin-Drumel, J. Van Wijingaarden, O. Zingsheim, F. Lewen, M. E. Harding, S. Schlemmer, S. Thorwirth, *J. Mol. Spectrosc.* **2015**, *307*, 33–39. [d] Observed band positions and relative intensities based on the integrated band areas in parentheses.

Table S3. Computed and observed IR frequencies (cm^{-1}) of *anti*-OSSO.

| computed[a] | | | | | observed[c] | | | mode |
| B3LYP/6-311+G(3df) | | CCSD(T)-F12b/VTZ-F12 | | MRCI/cc-pV(T+d)Z[b] | | | | |
normal	guess=mix	harmonic	anharmonic	harmonic	Ar-matrix	N$_2$-matrix	Ne-matrix	
1160 (0)	1133 (0)	1160	1148 (0)	1250 (0)				ν_1
1131 (378)	1116 (300)	1133	1122 (1552)	1231 (560)	1105.5	1102.8	1110.2	ν_2
580 (0)	428 (0)	571	561 (0)	584 (0)				ν_3
342 (0)	309 (0)	344	339 (0)	375 (0)				ν_4
192 (12)	179 (18)	187	186 (20)	209 (49)				ν_5
186 (20)	166 (11)	180	180 (55)	189 (0)				ν_6

[a] Computed IR intensities (km mol^{-1}) in parentheses. [b] B. N. Frandsen, P. O. Wennberg, H. G. Kjaergaard, *Geophys. Res. Lett.* **2016**, *43*, 11146–11155. [c] Observed band positions and relative intensities based on the integrated band areas in parentheses.

Table S4. Computed and observed IR frequencies (cm^{-1}) of *syn*-OSOS.

| computed[a] | | | | | observed[c] | | | mode |
| B3LYP/6-311+G(3df) | | CCSD(T)-F12b/VTZ-F12 | | MRCI/cc-pV(T+d)Z[b] | | | | |
normal	guess=mix	harmonic	anharmonic	harmonic	Ar-matrix	N$_2$-matrix	Ne-matrix	
1254 (172)	1213 (142)	1243	1237 (157)	1330 (250)	1209.3 (100)	1213.3 (100)	1210.0 (100)	ν_1
745 (50)	744 (11)	784	740 (837)	971 (410)	764.6 (6)	n.o.	770.7 (5)	ν_2
647 (25)	520 (12)	644	622 (88)	677 (69)				ν_3
514 (13)	493 (12)	515	508 (11)	538 (16)				ν_4
335 (13)	244 (10)	306	302 (18)	267 (0)				ν_5
151 (0.5)	164 (1)	173	172 (0.3)	194 (9)				ν_6

[a] Computed IR intensities (km mol^{-1}) in parentheses. [b] B. N. Frandsen, P. O. Wennberg, H. G. Kjaergaard, *Geophys. Res. Lett.* **2016**, *43*, 11146–11155. [c] Observed band positions and relative intensities based on the integrated band areas in parentheses.

Table S5. Computed and observed IR spectra of *cyclic*-OS(=O)S.

computed [a]					observed			mode
B3LYP/6-311+G(3df)		CCSD(T)-F12b/VTZ-F12		MRCI/cc-pV(T+d)Z[b]				
normal	guess=mix	harmonic	anharmonic		Ar-matrix	N$_2$-matrix	Ne-matrix	
1272 (217)	1272 (217)	1284	1266 (339)	1396 (560)	1252.3 (100)	1248.9 (100)	1259.9 (100)	ν_1
805 (46)	805 (46)	819	803 (58)	894 (95)	795.7 (23)	793.6 (21)	793.9 (18)	ν_2
559 (30)	559 (30)	570	559 (29)	593 (57)				ν_3
442 (29)	442 (29)	466	459 (55)	505 (76)				ν_4
414 (14)	414 (14)	422	417 (20)	462 (39)				ν_5
266 (0.3)	266 (0.3)	275	272 (0.8)	302 (2)				ν_6

[a] Computed IR intensities (km mol^{-1}) in parentheses. [b] B. N. Frandsen, P. O. Wennberg, H. G. Kjaergaard, *Geophys. Res. Lett.* **2016**, *43*, 11146–11155.

Table S6. Computed (B3LYP/6-311+G(3df)) and observed ^{18}O-isotopic shifts (cm^{-1}) of S_2O_2 isomers.

mode	*syn*-OSSO		*anti*-OSSO		*syn*-OSOS		*cyclic*-OS(=O)S	
	calculated	observed	calculated	observed	calculated	observed	calculated	observed
ν_1	44.0	42.8	41.6		45.1	45.9	47.0	43.0
ν_2	42.8	44.1	41.2	41.6	29.4	28.4	29.5	34.5
ν_3	1.8		5.4		9.9		17.5	
ν_4	11.7		8.5		21.0		6.9	
ν_5	7.3		7.4		9.3		16.9	
ν_6	7.3		6.9		5.7		8.7	

References:

(1) Hartzell, G. E.; Paige, J. N. *J. Am. Chem. Soc.* **1966**, *88*, 2616–2617.

(2) Howe, R. K.; Gruner, T. A.; Carter, L. G.; Black, L. L.; Franz, J. E. *J. Org. Chem.* **1978**, *43*, 3736–3742.

(3) Becke, A. D. *J. Chem. Phys.* **1993**, *98*, 5648–5652.

(4) a) Adler, T. B.; Knizia, G.; Werner, H.-J.; *J. Chem. Phys.* **2007**, *127*, 221106; b) Knizia, G.; Adler, T. B.; Werner, H.-J. *J. Chem. Phys.* **2009**, *130*, 054104; c) Peterson, K. A.; Adler,T. B.; Werner, H.-J. *J. Chem. Phys.* **2008**, *128*, 084102.

(5) a) Stratmann, R. E.; Scuseria, G. E.; Frisch, M. J. *J. Chem. Phys.* **1998**, *109*, 8218. b) Foresman, J. B.; Head-Gordon, M.; Pople, J. A.; Frisch, M. J. *J. Phys. Chem.* **1992**, *96*, 135.

(6) Frisch, M. J.; Trucks, G. W.; Schlegel, H. B.; Scuseria, G. E.; Robb, M. A.; Cheeseman, J. R.; Scalmani, G.; Barone, V.; Mennucci, B.; Petersson, G. A.; Nakatsuji, H.; Caricato, M.; Li, X.; Hratchian, H. P.; Izmaylov, A. F.; Bloino, J.; Zheng, G.; Sonnenberg, J. L.; Hada, M.; Ehara, M.; Toyota, K.; Fukuda, R.; Hasegawa, J.; Ishida, M.; Nakajima, T.; Honda, Y.; Kitao, O.; Nakai, H.; Vreven, T., Montgomery, Jr., J. A., Peralta, J. E., Ogliaro, F., Bearpark, M., Heyd, J. J., Brothers, E., Kudin, K. N.; Staroverov, V. N.; Kobayashi, R.; Normand, J.; Raghavachari, K.; Rendell, A.; Burant, J. C.; Iyengar, S. S.; Tomasi, J.; Cossi, M.; Rega, N.; Millam, N. J.; Klene, M.; Knox, J. E.; Cross, J. B.; Bakken, V.; Adamo, C.; Jaramillo, J.; Gomperts, R.; Stratmann, R. E.; Yazyev, O.; Austin, A. J.; Cammi, R.; Pomelli, C.; Ochterski, J. W.; Martin, R. L.; Morokuma, K.; Zakrzewski, V. G.; Voth, G. A.; Salvador, P.; Dannenberg, J. J.; Dapprich, S.; Daniels, A. D.; Farkas, Ö.; Foresman, J. B.; Ortiz, J. V.; Cioslowski, J.; Fox, D. J. Gaussian 09, A.1; Gaussian, Inc.: Wallingford CT, 2009.

(7) Werner, H. J.; Knowles, P. J.; Knizia, G.; Manby, F. R.; Schütz, M. *Wiley Interdiscip. Rev.: Comput. Mol. Sci.* **2012**, *2*, 242–3253.

(8) For examples, see: a) Pasinszki, T.; Kárpáti, T.; Westwood, N. P. C. *J. Phys. Chem. A* **2001**, *105*, 6258–6265; b) Franz, J. E.; Howe, R. K.; Pearl, H, K. *J. Org. Chem.* **1976**, *41*, 620–626; c) Kambouris, P.; Plisnier, M.; Flammang, R.; Terlouw, J. K.; Wentrup, C. *Tetrahedron Lett.* **1991**, *32*, 1487–1490.

Computed atomic coordinates (in Angstroms) and energies (in Hartrees).
syn-OSSO
B3LYP/6-311+G(3df)

O	1.64085500	0.88443500	0.00001000
O	-1.64079700	0.88448500	-0.00001000
S	1.00713100	-0.44222900	-0.00000800
S	-1.00716000	-0.44223100	0.00000800

Zero-point correction=	0.008475
Thermal correction to Energy=	0.012923
Thermal correction to Enthalpy=	0.013868
Thermal correction to Gibbs Free Energy=	-0.019779
Sum of electronic and zero-point Energies=	-946.887164
Sum of electronic and thermal Energies=	-946.882715
Sum of electronic and thermal Enthalpies=	-946.881771
Sum of electronic and thermal Free Energies=	-946.915418

B3LYP/6-311+G(3df)
anti-OSSO

S	0.00000000	1.01301700	0.00000000
O	-1.38041600	1.53669200	0.00000000
S	-0.00018900	-1.01396800	0.00000000
O	1.38079500	-1.53479100	0.00000000

Zero-point correction=	0.008178
Thermal correction to Energy=	0.012749
Thermal correction to Enthalpy=	0.013693
Thermal correction to Gibbs Free Energy=	-0.020027
Sum of electronic and zero-point Energies=	-946.882521
Sum of electronic and thermal Energies=	-946.877950
Sum of electronic and thermal Enthalpies=	-946.877005
Sum of electronic and thermal Free Energies=	-946.910725

syn-OSOS
B3LYP/6-311+G(3df)

O	0.35683900	-0.76717200	0.00039300
O	-1.40586300	1.04089300	0.00019100
S	1.68865200	0.24860900	-0.00009700
S	-1.16414000	-0.38546900	-0.00019500

Zero-point correction=	0.008305
Thermal correction to Energy=	0.012617
Thermal correction to Enthalpy=	0.013562
Thermal correction to Gibbs Free Energy=	-0.019809
Sum of electronic and zero-point Energies=	-946.851167
Sum of electronic and thermal Energies=	-946.846855
Sum of electronic and thermal Enthalpies=	-946.845910
Sum of electronic and thermal Free Energies=	-946.879281

anti-OSOS
B3LYP/6-311+G(3df)

O	0.00000000	0.57299700	0.00000000
O	2.05418000	-0.80692500	0.00000000
S	-1.63606200	0.99110200	0.00000000
S	0.60897200	-0.87413800	0.00000000

Zero-point correction= 0.007703
Thermal correction to Energy= 0.012320
Thermal correction to Enthalpy= 0.013264
Thermal correction to Gibbs Free Energy= -0.020481
Sum of electronic and zero-point Energies= -946.842254
Sum of electronic and thermal Energies= -946.837637
Sum of electronic and thermal Enthalpies= -946.836692
Sum of electronic and thermal Free Energies= -946.870437

cyclic OS(=O)S
B3LYP/6-311+G(3df)

O	0.38712400	1.08690800	-0.27586300
O	-1.67964800	-0.42572400	-0.48783100
S	1.32948800	-0.39438600	-0.04740300
S	-0.68322600	0.06379400	0.42925000

Zero-point correction= 0.008559
Thermal correction to Energy= 0.012697
Thermal correction to Enthalpy= 0.013642
Thermal correction to Gibbs Free Energy= -0.019004
Sum of electronic and zero-point Energies= -946.869690
Sum of electronic and thermal Energies= -946.865553
Sum of electronic and thermal Enthalpies= -946.864608
Sum of electronic and thermal Free Energies= -946.897254

SSO_2
B3LYP/6-311+G(3df)

O	-1.11105800	1.23598900	0.00006500
O	-1.11140200	-1.23581200	0.00006600
S	1.49633900	-0.00007900	-0.00006700
S	-0.38510900	-0.00000900	0.00000200

Zero-point correction= 0.010119
Thermal correction to Energy= 0.014022
Thermal correction to Enthalpy= 0.014966
Thermal correction to Gibbs Free Energy= -0.017404
Sum of electronic and zero-point Energies= -946.896700
Sum of electronic and thermal Energies= -946.892797
Sum of electronic and thermal Enthalpies= -946.891853
Sum of electronic and thermal Free Energies= -946.924223